

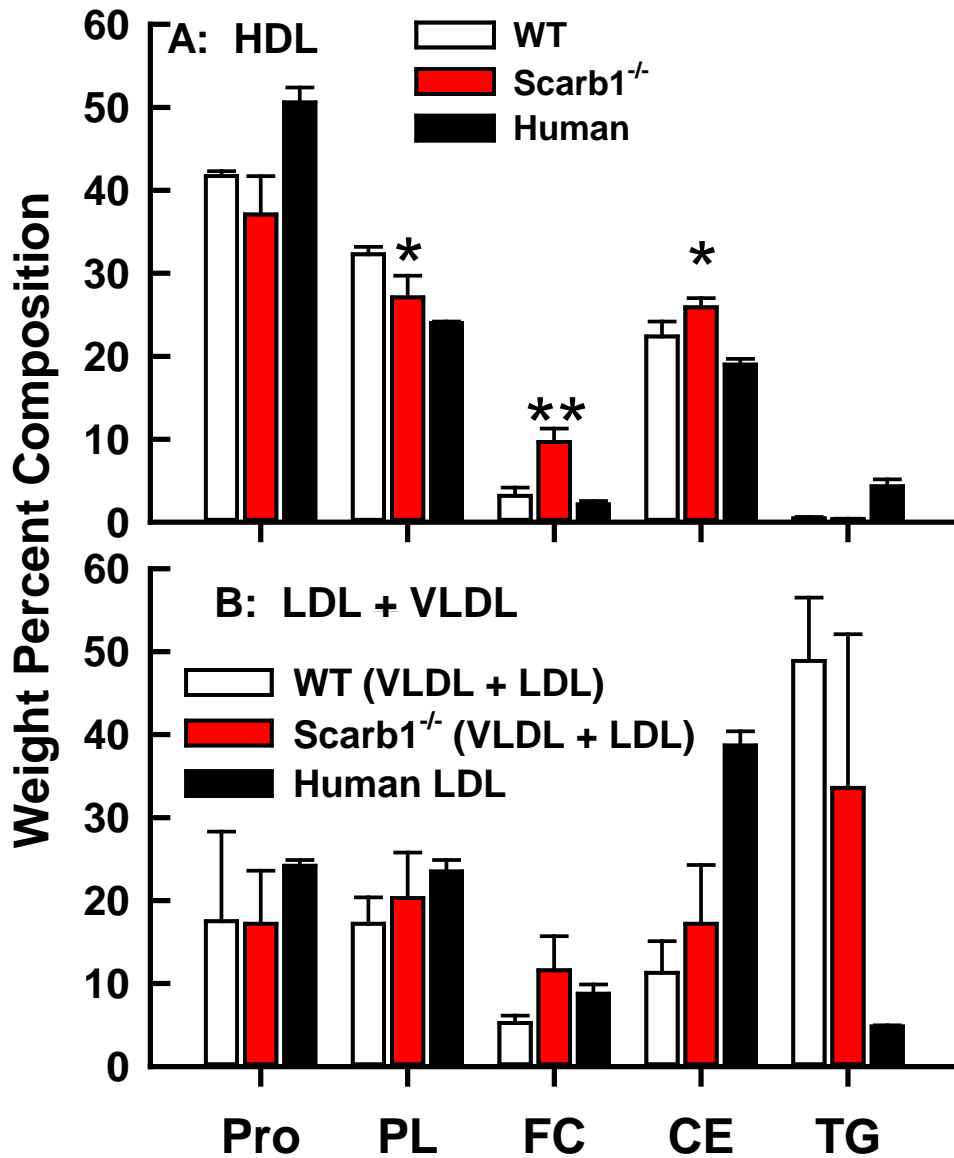
# Supplemental Materials

Jing Liu,<sup>1,2</sup> Baiba K. Gillard,<sup>2,3\*</sup> Dedipya Yelamanchili,<sup>2</sup>

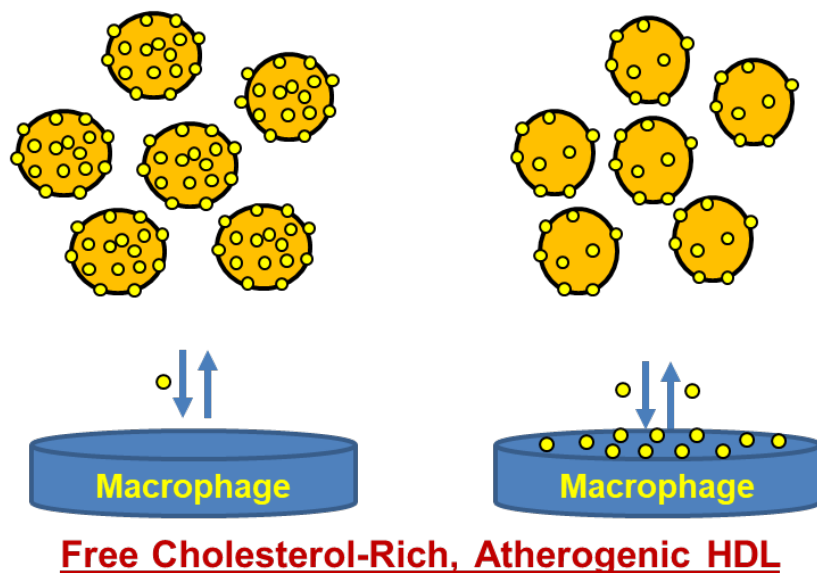
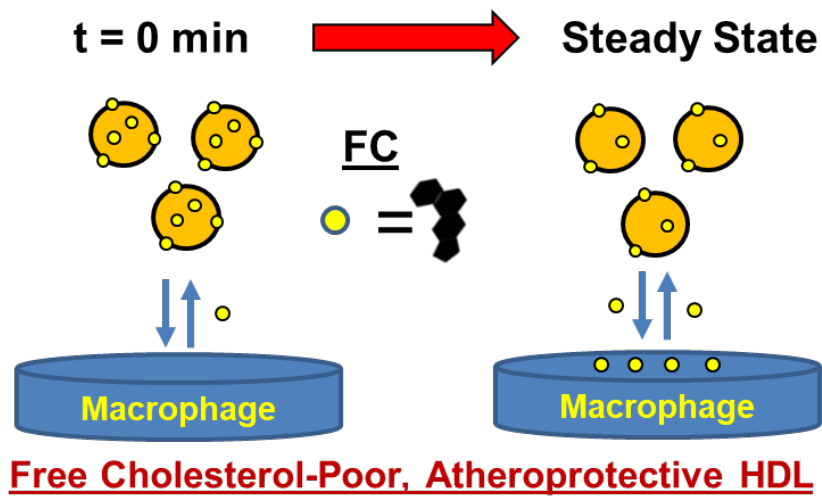
Antonio M. Gotto Jr.,<sup>2,3</sup> Corina Rosales,<sup>2,3</sup> and Henry J. Pownall<sup>2,3\*</sup>

*High Free Cholesterol Bioavailability Drives the Tissue Pathologies in Scarb1<sup>-/-</sup> Mice*

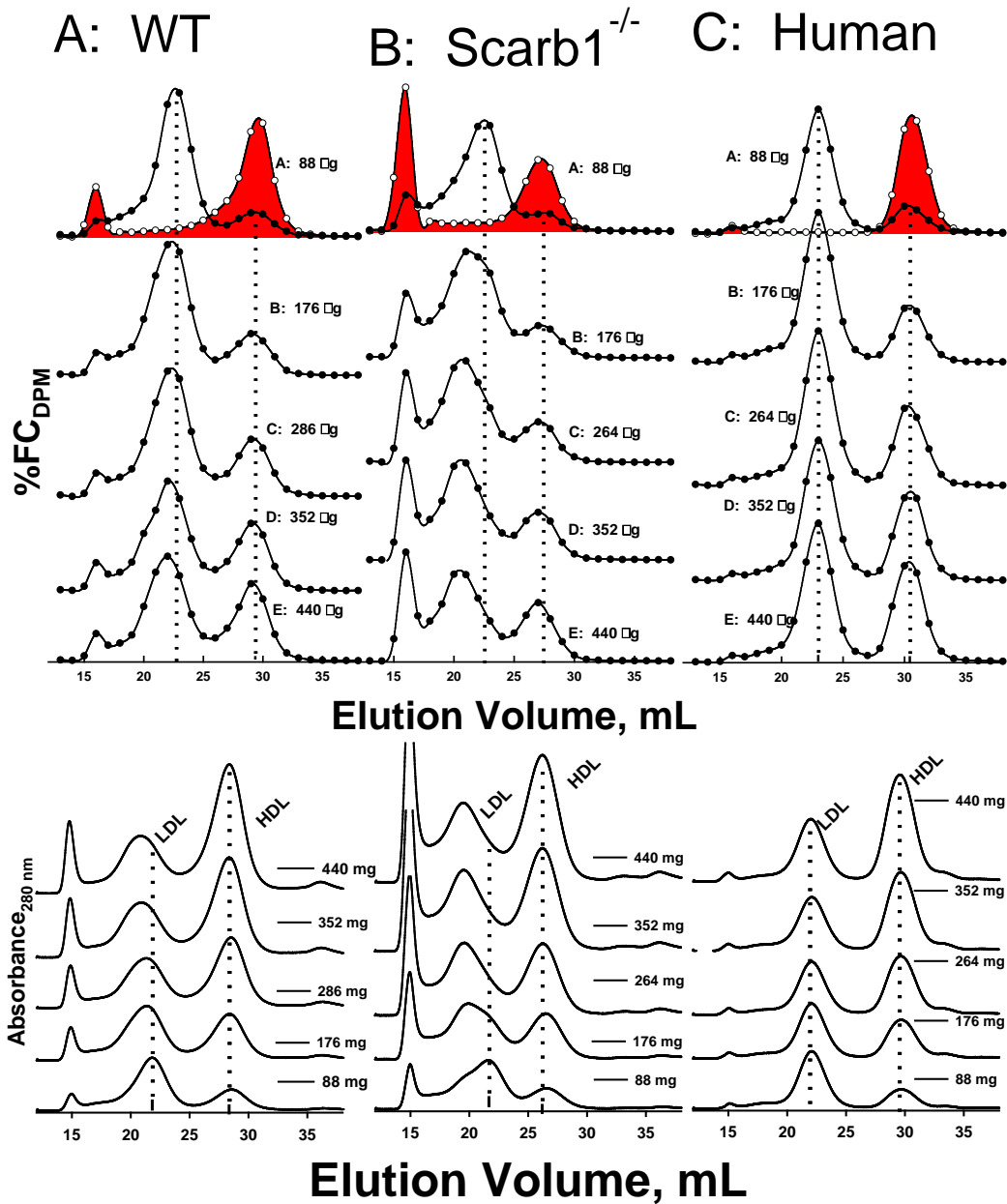
<sup>1</sup>Department of Cardiovascular Medicine, Xiangya Hospital, Central South University, Changsha 410008, China, <sup>2</sup>Center for Bioenergetics, Houston Methodist Research Institute, 6670 Bertner Avenue, Houston TX 77030, USA; <sup>3</sup>Department of Medicine, Weill Cornell Medicine, 1300 York Ave, New York, NY, 10065, USA.



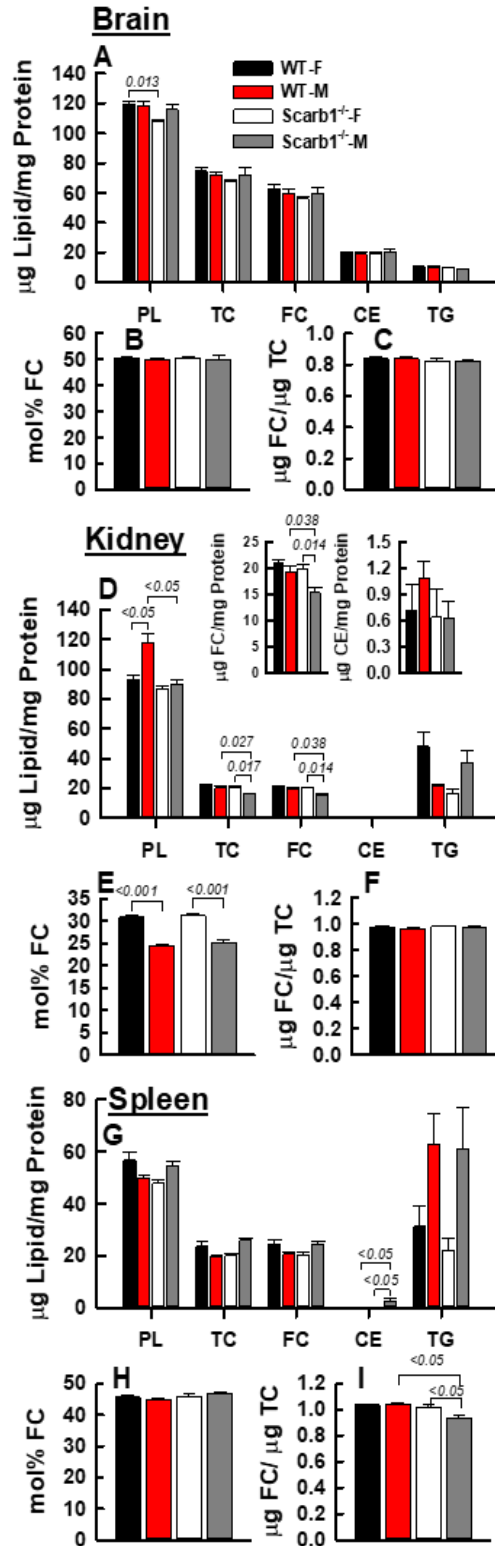
**Supplementary Figure I:** Lipoprotein Compositions. A) Human and Scarb1<sup>-/-</sup> mouse HDL. B) Human LDL and Scarb1<sup>-/-</sup> and WT mouse (VLDL + LDL). \*P < 0.05 for Scarb1<sup>-/-</sup> vs. WT lipoprotein. \*\*P < 0.001 Scarb1<sup>-/-</sup> vs. WT. This bar graph was created from the data in Supplementary Table 1.



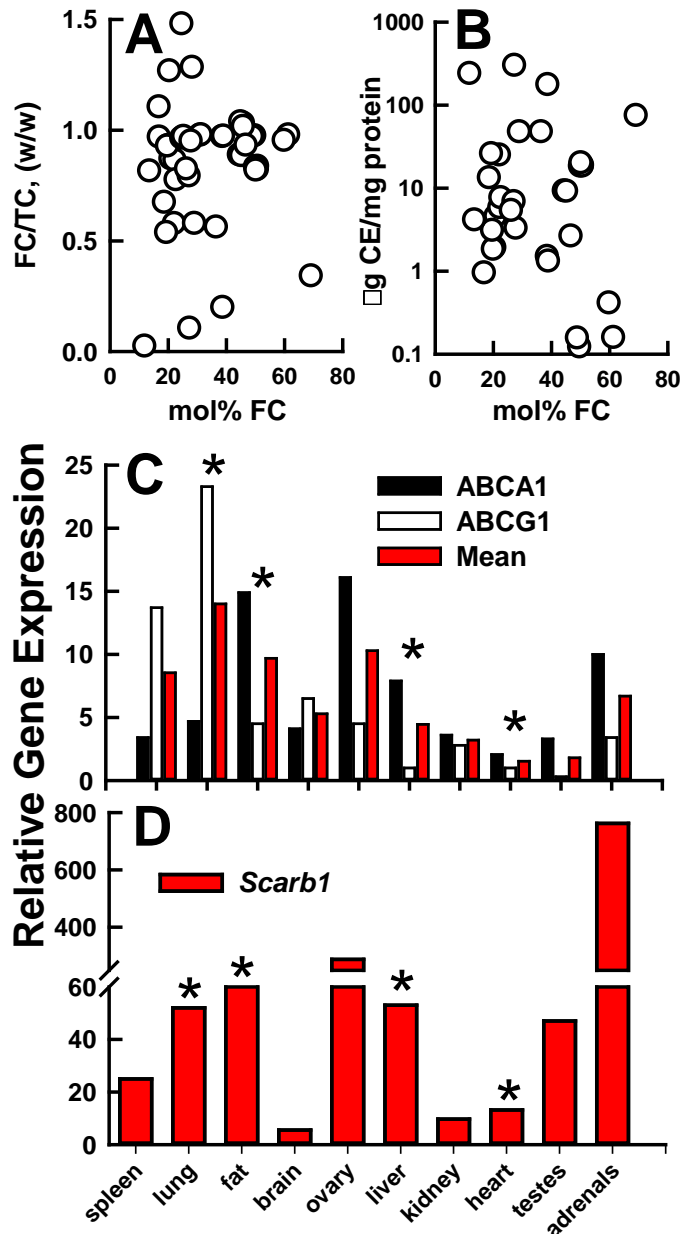
**Supplementary Figure II:** Hypothetical Mechanism by which HDL-FC Bioavailability Drives FC Transfer into other Lipid Surfaces. Kinetic model compares FC transfer from FC-poor and -rich HDL. Relative numbers of FC on the surfaces for FC-poor and rich HDL are proportional to the reported values for WT and Scarb1<sup>-/-</sup> mouse HDL. FC distribution is shown at t = 0 and at steady state as labeled.



**Supplementary Figure III.** Extent of [<sup>3</sup>H]FC transfer from HDL of WT mice (A), *Scarb1*<sup>-/-</sup> mice (B), and humans (C) (88 to 440 μg protein/220 μL) to human LDL (176 μg protein/220 μL) at equilibrium as determined by SEC. Top panels: [<sup>3</sup>H] FC dpm, bottom panels Absorbance<sub>280nm</sub>. Red chromatograms in the topmost panels (A: 88 μg HDL) are the SEC profiles for the starting radiolabeled HDL.



**Supplementary Figure IV:** Lipid Compositions of Brain, Kidney, and Spleen of Male (M) and Female (F) WT and *Scarb1*<sup>-/-</sup> Mice. Tissue sites are as labeled. Bars are mean  $\pm$  SEM. Numbers of mice per group for all three tissues are: WT-F (n = 12), WT-M (n = 10), *Scarb1*<sup>-/-</sup>-F (n = 11) and *Scarb1*<sup>-/-</sup>-M (n = 5). Statistics as in Methods and **Figure 1** legend. P values for significant differences ( $p < 0.05$ ) for comparison of WT vs. *Scarb1*<sup>-/-</sup> mice of the same sex, and M vs. F of the same genotype are shown.



**Supplementary Figure V.** Correlation of tissue FC/TC ratio (A) and CE/protein ratio (B) vs. mol% FC. Data from **Supplementary Table III**. C. Tissue expression of cholesterol transporters ABCA1 and ABCG1. D. Tissue expression of SCARB1. \*Denotes tissues that are FC-enriched among *Scarb1*<sup>-/-</sup> vs. WT mice. The data show that there is not pattern of all-high or all-low expression of ABCA1, ABCG1, and *Scarb1* that associates with FC-enrichment. Gene expression data are from <https://www.ncbi.nlm.nih.gov/gene>.

**Supplementary Table I: Lipoprotein Compositions (weight %)<sup>a</sup>**

	n	Pro	PL	FC	CE	TG	Mol% FC
<b>HDL</b>							
WT Mice	4	41.7 ± 0.6	32.3 ± 0.9	3.18 ± 1.01	22.4 ± 1.8	0.43 ± 0.18	16.0 ± 4.3
Scarb1 <sup>-/-</sup> Mice	4	37.1 ± 4.6	27.1 ± 2.6	9.67 ± 1.61	25.9 ± 1.1	0.36 ± 0.05	41.1 ± 2.4
Human	2	50.6 ± 1.8	24.0 ± 0.2	2.15 ± 0.41	19.0 ± 0.7	4.34 ± 0.82	15.0 ± 2.5
<i>t-test p<sup>b</sup></i>		0.087	0.010	0.000	0.017	0.467	0.000
<b>VLDL+LDL</b>							
WT Mice	3	17.5 ± 10.8	17.2 ± 3.2	5.25 ± 0.89	11.3 ± 3.8	48.9 ± 7.6	37.6 ± 1.4
Scarb1 <sup>-/-</sup> Mice	3	17.2 ± 6.4	20.3 ± 5.5	11.60 ± 4.1	17.2 ± 7.1	33.6 ± 18.5	52.5 ± 2.0
Human LDL	2	24.2 ± 0.7	23.5 ± 1.4	8.79 ± 1.09	38.7 ± 1.7	4.83 ± 0.13	42.3 ± 1.6
<i>t-test p<sup>b</sup></i>		0.973	0.438	0.059	0.269	0.257	0.000

<sup>a</sup>Mouse HDL and VLDL + LDL lipoproteins were purified from n pools of plasma from 5 - 10 mice each. Human HDL and LDL were from individual donors. Values are mean ± SD. Pro = protein, PL = phospholipid, FC = free cholesterol, CE = cholesteryl ester, TG = triglyceride. <sup>b</sup> Student t-test p value, WT vs Scarb1<sup>-/-</sup> mice.

**Supplementary Table II: Kinetic Constants for FC Flux between HDL and J774 Macrophages<sup>a</sup>**

FC Influx					
HDL	Time Course			Dose Response	
	$k_i$ (initial influx) <i>nmol FC influx/mg cell-protein/min</i>	$k$ , $min^{-1}$	$Influx_{max}$ <i>nmol FC/mg cell-protein</i>	$Influx_{max}$ <i>nmol FC/mg cell-protein</i>	$Influx_{50\%}$ <i>μg HDL-protein/mL</i>
Scarb1 <sup>-/-</sup>	0.098	0.020 ± 0.001	4.9 ± 0.11	26.7 ± 0.7	113 ± 5
WT	0.024	0.019 ± 0.001	1.2 ± 0.02	8.7 ± 0.6	150 ± 14
Human	0.033	0.012 ± 0.002	2.7 ± 0.17	18.3 ± 4.8	136 ± 52
FC Efflux					
HDL	Time Course			Dose Response	
	$k_e$ (initial efflux), <i>nmol FC efflux/mg cell-protein/min</i>	$k$ , $min^{-1}$	$Efflux_{max}$ <i>nmol FC/mg cell-protein</i>	$Efflux_{max}$ <i>nmol FC/mg cell-protein</i>	$Influx_{50\%}$ <i>μg HDL-protein/mL</i>
Scarb1 <sup>-/-</sup>	0.139	0.018 ± 0.004	7.6 ± 0.9	32.3 ± 2.0	72.1 ± 7.9
WT	0.154	0.019 ± 0.006	8.3 ± 1.1	37.1 ± 2.7	81.2 ± 10.4
Human	0.124	0.016 ± 0.005	7.6 ± 1.1	34.4 ± 3.0	81.8 ± 12.2

<sup>a</sup> Rate constants and maximum influx and efflux values were calculated by exponential and hyperbolic fits to the time course and dose response data of **Figure 2 G - J**. Initial rate constants  $k_i$  and  $k_e$  are calculated from the initial slope of the time course, while  $k$  values and influx and efflux maximum and 50% values are from the fit of the data over the entire time course or dose response. Errors are the standard errors for the regression analyses.



**Supplementary Table III: Tissue mol% FC and CE Content in WT vs. Scarb1<sup>-/-</sup> and Male vs. Female mice.<sup>a</sup>**

Tissue	Mol% Tissue FC				CE Content, µg/mg protein			
	WT		Scarb1 <sup>-/-</sup>		WT		Scarb1 <sup>-/-</sup>	
	Female	Male	Female	Male	Female	Male	Female	Male
Plasma*	34.1±2.0 (12)	27.9±3.4 (10)	<b>57.7±1.8<sup>†</sup></b> (11)	<b>65.9±1.3<sup>†</sup></b> (5)	1.23±0.05 (12)	<b>1.91±0.10<sup>‡</sup></b> (10)	<b>2.54±0.08<sup>†</sup></b> (11)	<b>2.51±0.13<sup>†</sup></b> (5)
HDL*	21.4±1.3 (12)	22.4±2.6 (10)	<b>59.4±3.2<sup>†</sup></b> (11)	<b>61.0±1.6<sup>†</sup></b> (5)	1.23±0.05 (12)	<b>1.79±0.10<sup>‡</sup></b> (10)	<b>2.18±0.12<sup>†</sup></b> (11)	<b>2.26±0.14<sup>†</sup></b> (5)
Erythrocytes	49.6±0.4 (6)	48.8±0.5 (4)	<b>61.2±0.7<sup>†</sup></b> (6)	<b>59.7±0.5<sup>†</sup></b> (8)	0.12±0.03 (6)	0.16±0.04 (4)	0.16±0.06 (6)	<b>0.42±0.05<sup>†‡</sup></b> (8)
Heart	16.8±0.2 (12)	16.7±0.5 (10)	<b>20.4±0.3<sup>†</sup></b> (11)	<b>20.2±0.6<sup>†</sup></b> (5)	0.97±0.99 (12)	bd (10)	1.95±0.93 (11)	bd (5)
Lung	38.4±0.4 (12)	38.8±0.3 (10)	<b>44.3±0.8<sup>†</sup></b> (11)	<b>45.1±0.7<sup>†</sup></b> (5)	1.53±0.59 (12)	1.34±0.55 (10)	<b>9.39±1.51<sup>†</sup></b> (11)	<b>9.32±1.00<sup>†</sup></b> (5)
Liver	19.8±0.4 (12)	20.8±0.6 (10)	<b>22.1±0.5<sup>†</sup></b> (11)	<b>19.6±0.2<sup>‡</sup></b> (5)	1.86±0.98 (12)	4.63±1.31 (10)	5.90±1.96 (11)	3.14±3.01 (5)
Abdominal Fat	27.7±3.3 (4)	22.0±2.4 (5)	28.1±1.4 (4)	<b>36.4±3.3<sup>†</sup></b> (5)	3.3±4.7 (4)	<b>25.5±3.2<sup>‡</sup></b> (5)	bd (4)	<b>48.4±9.6<sup>‡</sup></b> (5)
Ovarian Fat	24.5±1.2 (5)		22.5±1.2 (4)		bd (5)		<b>7.77±4.2<sup>†</sup></b> (4)	
Testes Fat		13.4±1.4 (5)		<b>19.3±2.7<sup>†</sup></b> (5)		4.19±1.1 (5)		<b>26.3±5.8<sup>†</sup></b> (5)
Ovaries	38.6±3.7 (12)		<b>69.0±2.3<sup>†</sup></b> (8)		<b>179.3±9.4 (12)</b>		<b>76.0±6.3<sup>†</sup></b> (8)	
Testes		27.0±0.3 (10)		26.1±0.2 (5)		7.0±0.6 (10)		5.5±0.4 (5)
Adrenals	27.2±0.4 (3)	<b>11.7±5.9 (3)<sup>‡</sup></b>	28.9±6.0 (3)	<b>18.5±1.2 (7)<sup>‡</sup></b>	<b>305.1±5.5 (3)</b>	<b>244.3±19.8 (3)<sup>‡</sup></b>	<b>48.5±16.1 (3)<sup>†</sup></b>	<b>13.5±1.0 (7)<sup>†‡</sup></b>
Brain	50.6±0.7 (12)	49.8±0.5 (10)	50.5±0.4 (11)	50.0±1.3 (5)	19.1±1.4 (12)	18.7±1.1 (10)	19.0±1.3 (11)	20.5±1.3 (5)
Kidney	30.8±0.4 <sup>‡</sup> (12)	<b>24.4±0.4<sup>‡</sup></b> (10)	31.1±0.4 <sup>‡</sup> (11)	<b>25.2±0.6<sup>‡</sup></b> (5)	0.73±0.30 (12)	1.09±0.19 (10)	0.64±0.33 (11)	0.64±0.19 (5)
Spleen	45.7±0.7 (12)	44.8±0.7 (10)	45.7±0.8 (11)	46.6±0.5 (5)	bd	bd	bd	2.68±0.7 <sup>†‡</sup> (5)

<sup>a</sup>Values are mean ± (SEM). Number of mice per group is given in parentheses (n). Red font, Scarb1<sup>-/-</sup> values differ from WT; blue font, male vs. female values differ; bd, below detection limit.

\*Plasma and HDL CE values are mg CE/mL plasma.

<sup>†</sup>Values significantly different between genotypes for the same sex, p<0.05.

<sup>‡</sup>Values significantly different between sexes for the same genotype, p<0.05.

<sup>‡</sup>p<0.10 for Scarb1<sup>-/-</sup> M vs WT-M, and for WT-M vs -F for abdominal fat CE, and for WT-M vs -F adrenal mol % FC.

**Supplementary Table IV: Kinetic Constants for HDL-[<sup>3</sup>H]FC Clearance In Vivo\***

Genotype/Sex	k <sub>i</sub> , %/min	k <sub>1</sub> , min <sup>-1</sup>	t <sub>1/2</sub> , min	Final % DPM	ΔHDL-FC, mg/mL/min	FCR, pools/min*
WT Female	42.8 ± 1.6	1.27 ± 0.28	0.6	7.5 ± 1.8	0.055	1.16
WT Male	35.3 ± 2.0 <sup>†</sup>	0.72 ± 0.07	1.1	8.9 ± 1.5	0.070	0.63
Scarb1 <sup>-/-</sup> Female	26.9 ± 1.7 <sup>‡</sup>	0.86 ± 0.59	1.9	37 ± 6	0.28	0.36
Scarb1 <sup>-/-</sup> Male	20.8 ± 1.8 <sup>†‡</sup>	0.59 ± 0.38	3.0	40 ± 7	0.28	0.23

\*Rate constants were from a fit of the data in **Figure 6**, where k<sub>i</sub> is the initial rate constant, k<sub>1</sub> is the rate constant from the exponential fit of the data over 0 – 90 minutes, t<sub>1/2</sub> = ln2/k<sub>1</sub>, and Final %DPM is the asymptote of the exponential fit (**Figure 6**). Initial ΔHDL-FC is the initial %change/min (**Figure 6**) times the plasma HDL-C concentration (**Figure 1**). FCR (fractional catabolic rate) = 0.693/t<sub>1/2</sub>. Standard errors are from the regression analyses.

<sup>†</sup>Male vs Female, p<0.02. <sup>‡</sup>

<sup>‡</sup>Scarb1<sup>-/-</sup> vs WT, p<0.001.

**Supplementary Table V: Differences in Tissues Compositions and Plasma Kinetics according to Sex\***

<b>Analyte</b>	<b>Comparison by Sex</b>
Plasma-PL	WT M > WT F
Plasma-CE	WT M > WT F
HDL-CE	WT M > WT F
Erythrocyte-PL	Scarb1 <sup>-/-</sup> M > Scarb1 F
Erythrocyte-TC	Scarb1 <sup>-/-</sup> M > Scarb1 F
Erythrocyte-FC	Scarb1 <sup>-/-</sup> M > Scarb1 F
Erythrocyte-CE	Scarb1 <sup>-/-</sup> M > Scarb1 F
Erythrocyte-FC/TC	Scarb1 <sup>-/-</sup> M < Scarb1 F
Heart-TC	Scarb1 <sup>-/-</sup> M < Scarb1 F
Heart-CE	Scarb1 <sup>-/-</sup> M < Scarb1 F
Heart-FC/TC	Scarb1 <sup>-/-</sup> M > Scarb1 F
Lung-PL	WT M < WT F
Lung-FC	WT M < WT F
Liver-PL	Scarb1 <sup>-/-</sup> M < Scarb1 F
Liver-TC	Scarb1 <sup>-/-</sup> M < Scarb1 F
Liver-FC	Scarb1 <sup>-/-</sup> M < Scarb1 F
Liver-TG	Scarb1 <sup>-/-</sup> M < Scarb1 F
Liver-mol% FC	Scarb1 <sup>-/-</sup> M < Scarb1 F
Abdominal Fat-PL	Scarb1 <sup>-/-</sup> M > Scarb1 F
Abdominal Fat-TC	Scarb1 <sup>-/-</sup> M > Scarb1 F
Abdominal Fat-CE	Scarb1 <sup>-/-</sup> M > Scarb1 F
Abdominal Fat-FC/TC	Scarb1 <sup>-/-</sup> M < Scarb1 F
Adrenal-PL	Scarb1 <sup>-/-</sup> M < Scarb1 F; WT M < WT F
Adrenal-TC	Scarb1 <sup>-/-</sup> M < Scarb1 F; WT M < WT F
Adrenal-FC	Scarb1 <sup>-/-</sup> M < Scarb1 F; WT M < WT F
Adrenal-CE	Scarb1 <sup>-/-</sup> M < Scarb1 F; WT M < WT F
Adrenal-mol% FC	Scarb1 <sup>-/-</sup> M < Scarb1 F; WT M < WT F
Adrenal FC/TC	WT M < WT F
Kidney-PL	WT M > WT F
Kidney-TC	Scarb1 <sup>-/-</sup> M < Scarb1 F
Kidney-FC	Scarb1 <sup>-/-</sup> M < Scarb1 F
Kidney-mol% FC	Scarb1 <sup>-/-</sup> M < Scarb1 F; WT M < WT F
Spleen-CE	Scarb1 <sup>-/-</sup> M > Scarb1 F
Spleen-FC/TC	Scarb1 <sup>-/-</sup> M < Scarb1 F
Plasma FC clearance rate	Scarb1 <sup>-/-</sup> M < Scarb1 F; WT M < WT F

\*Red and black font distinguish F vs. M significant differences among Scarb1<sup>-/-</sup> vs. WT mice respectively.

## Supplementary Table VI: Major Resources

### Animals (in vivo studies)

Species	Vendor or Source	Background Strain	Sex	Persistent ID / URL
Mus musculus	The Jackson Laboratory	B6;129S-Scarb1tm1Kri/J and WT C57BL/6J	M & F	<a href="#">JAXMice Search</a>

### Cultured Cells

Name	Vendor or Source	Sex (F, M, or unknown)	Persistent ID / URL
J774 macrophages	American Tissue Culture Collection	NA	<a href="#">ATCC: The Global Bioresource Center</a>

## Materials and Methods

*Disclosure:* The data that support the findings of this study are available from the corresponding author upon reasonable request.

*Lipoprotein Isolation:* Lipoproteins were isolated from pooled mouse plasma (5-10/genotype) by sequential flotation.<sup>1,2</sup> Purity was verified by size exclusion chromatography (SEC)<sup>3</sup> and compositional analyses. HDL from individual mice was isolated by heparin-manganese precipitation of plasma APOB lipoproteins.<sup>4,5</sup> Plasma and tissue lipids were determined using enzyme-based assays for FC, total cholesterol (TC), PL, and triglyceride (TG) (Fujifilm Wako Diagnostics Inc.). Cholesterol ester (CE) concentrations were calculated as (mg TC - mg FC) x 1.6. . Protein was determined by the DC Protein Assay (Bio-Rad, Inc.).

*In Vitro HDL-FC Transfer Kinetics:* HDL was radiolabeled with [<sup>3</sup>H]FC as described previously.<sup>6</sup> In brief, [<sup>3</sup>H]FC in ethanol was transferred to filter paper (~1 cm<sup>2</sup>) and the solvent evaporated. The labeled filter paper was transferred to incubation buffer (TBS; 10 mM Tris, 100 mM NaCl, containing 1 mg protein/mL of WT, Scarb1<sup>-/-</sup> or human HDL and incubated at 4 °C overnight. The filter paper was then removed. Specific activities (dpm/nmoles FC) were calculated on the basis of HDL-FC concentration and β-counting of aliquots in triplicate. According to SEC, HDL-absorbance (280 nm) and radiolabel co-eluted. To assay rates of transfer of HDL-FC to LDL, HDL-[<sup>3</sup>H]FC (10 μg protein/mL) was incubated with human LDL (1.0 mg/mL) at 37 °C. Aliquots were removed over time (0 – 20 min) and LDL precipitated with heparin-Mn<sup>2+</sup>.<sup>4,5</sup> Supernatants containing HDL were β-counted and counts vs. time data from two independent experiments were combined and fitted to a three-parameter exponential decay equation from which transfer rate constants and the asymptote, i.e., the equilibrium [<sup>3</sup>H]FC transferred to LDL, were extracted.

*Equilibrium Distribution of [<sup>3</sup>H]FC between LDL and HDL:* Given that HDL-[<sup>3</sup>H]FC spontaneously transfers to LDL with t<sub>1/2</sub> ~5 min,<sup>4</sup> we measured the concentration-dependence of this process at equilibrium by incubating human LDL (0.8 mg protein/mL) and various concentrations of HDL-[<sup>3</sup>H]FC (0.4 to 2.0 mg protein/mL) for ~18 h at 37 °C. At the end of the incubations, aliquots were passed over a size exclusion column, which separates HDL from LDL. The eluted fractions were collected and β-counted, and the mass of [<sup>3</sup>H]FC transferred from HDL to LDL was based on the radioactivity eluting with LDL. Genotype-dependent differences in the HDL-[<sup>3</sup>H]FC to LDL transfer were determined by comparing the slopes of a linear regression analysis of LDL-associated FC mass vs. the HDL-protein and HDL-FC concentrations in the incubation.

*FC Flux between HDL and Macrophages:* FC flux between HDL and J774 macrophages (J774A.1, ATCC® TIB67™) were measured essentially as described.<sup>3, 7-10</sup> To quantify FC influx, [<sup>3</sup>H]FC-labeled HDL was incubated with macrophages and cell-associated [<sup>3</sup>H]FC was measured as a function of HDL concentration and time.<sup>3, 10</sup> Cells were seeded in 12-well plates and each assay point was performed in triplicate. At various incubation times, media were collected, and the cells washed three times with cold buffer. Cell lipids were twice extracted with isopropanol and the extracts β-counted. Residual cells were solubilized in 1 mL NaOH (0.1 M) and the protein quantified (BioRad DC). Influx dose-response was assayed at 2 h and analyzed using a two-parameter hyperbolic function, Influx (FC/mg cell-protein) =  $\frac{ac}{(b + c)}$ , where  $\frac{c}{b}$  is HDL concentration,  $\frac{a}{b}$  is maximum uptake, and  $\frac{c}{b}$ , the HDL concentration that produces 50% of maximum uptake, is a measure of influx power. For time course experiments, [<sup>3</sup>H]FC-labeled HDL (20 μg/mL) was incubated with macrophages for various times. Lipid

extraction and protein assays were performed as above. Uptake kinetics were fitted to a rising exponential function,  $\text{Influx (FC/mg cell-protein)} = a(1 - e^{-kt})$ , where  $t$  is time,  $k$  is the rate constant, and  $a$  is maximum uptake.

FC efflux to HDL was measured by incubating HDL with [ $^3\text{H}$ ]FC-labeled macrophages as described.<sup>7</sup> J774 macrophages were seeded at  $0.2 \times 10^6$  cells/ $3.8\text{cm}^2$ , grown to 40% confluency and radiolabeled with [ $^3\text{H}$ ]FC (0.5  $\mu\text{Ci/well}$ ). The media were removed, and the cells washed. For dose-response, HDL (10-100  $\mu\text{g HDL protein/mL}$ ) was added to the media, cells were incubated for 2 h, and for time course experiments the HDL concentration was 20  $\mu\text{g protein/mL}$ , after which media and washed cells were collected. The media were centrifuged (5 min @ 13,200 rpm) to remove cell debris and  $\beta$ -counted. Cell lipids were  $\beta$ -counted, and cell protein determined as above. Respective time- and concentration-dependence of efflux were fitted to exponential and hyperbolic equations as described for influx. Initial rates of influx and efflux were determined from the fitted time-course equations.

*Mouse Management and Tissue Analysis:* *Scarb1*<sup>-/-</sup> and WT C57BL/6J-mice (The Jackson Laboratory) were maintained on normal laboratory diet (Teklad Envigo Cat 2920). All were studied at 12-25 weeks of age except those analyzed for adrenal lipid compositions, which were 8-40 weeks old. Numbers of mice used for the various analyses are given in the Figure and Table legends. All mouse procedures complied with the National Institutes of Health Guide for the Care and Use of Laboratory Animals and were approved by the Institutional Animal Care and Use Committee. Retro-orbital injections of HDL- $^3\text{H}$ ]FC were conducted immediately after a one-time isoflurane inhalation (2.5%, 3-5 minutes) to achieve an anesthetic effect. WT and *Scarb1*<sup>-/-</sup> mice were euthanized and their blood collected by heart puncture into EDTA; tissues were harvested for lipid and protein analyses.<sup>11-13</sup> Tissues were weighed, homogenized, and extracted (hexane:2-propanol:acetic acid:3:2:1% v/v/v). Tissue-protein was solubilized with 0.4M NaOH + 1% sodium dodecyl sulfate. Extracted lipids were dissolved in 1% Triton in chloroform, the chloroform evaporated under nitrogen, and the lipids solubilized in water. Compositions were expressed as lipid mass/protein mass.

*In Vivo HDL-FC Metabolism:* HDL-FC turnover kinetics were determined in WT and *Scarb1*<sup>-/-</sup> mice (The Jackson Laboratory) as described.<sup>6</sup> Mice ( $n = 3-4/\text{time point}$ ) were retro-orbitally injected with HDL- $^3\text{H}$ ]FC, and euthanized at various times post-injection. Blood was collected and centrifuged to sediment cells, and the plasma from the supernatant was  $\beta$ -counted. Erythrocytes were washed, lipid-extracted, and protein determined as above. Kinetic data were fitted to a two-parameter exponential function of percent injected dose vs. time; initial rates were calculated as the percent change/min between  $t = 0$  and 2 min.

*Statistical Analysis:* Data, presented as mean  $\pm$  standard deviation (SD) or standard error of the mean (SEM) are given in Table and Figure legends. Group means were compared by Student's t-test in Prism 8.0 or Microsoft Excel (Office 16). Linear and non-linear regression analyses were done using SigmaPlot 12.0 and Prism 8.0. Prism was used to compare linear regression slopes and intercepts, including log transformed data for exponential decay fits. Differences in the plasma, lipoprotein, and tissue lipid compositions of WT male and female vs. *Scarb1*<sup>-/-</sup> male and female mice were identified by pairwise comparisons when the analysis of variance (SigmaPlot 12.0) on all four groups indicated significant differences,  $p < 0.05$ . Data were tested for normality (Shapiro-Wilk) and Equal Variance, and if passed, pairwise comparisons between groups were done using the All Pairwise Multiple Comparison Procedures (Holm-Sidak method) or Student's t-test. If the data failed normality or equal variance tests, the Kruskal-Wallis one-

way analysis of variance on ranks or a rank-sum test were used for pairwise comparisons and calculation of p values. Because in some tissues, lipid values for male and female mice of the same genotype differed, for pairwise comparisons of genotypes, we report only comparisons for the same sex, i.e. WT-F vs Scarb1<sup>-/-</sup>-F and WT-M vs Scarb1<sup>-/-</sup>-M. P < 0.05, which was considered significant, are given in the tables and figure legends. Data for human HDL when provided is for comparison and was not statistically evaluated.

1. Havel RJ, Eder HA and Bragdon JH. The distribution and chemical composition of ultracentrifugally separated lipoproteins in human serum. *J Clin Invest.* 1955;34:1345-53.
2. Schumaker VN and Puppione DL. Sequential flotation ultracentrifugation. *Methods Enzymol.* 1986;128:155-70.
3. Gillard BK, Rosales C, Pillai BK, Lin HY, Courtney HS and Pownall HJ. Streptococcal serum opacity factor increases the rate of hepatocyte uptake of human plasma high-density lipoprotein cholesterol. *Biochemistry.* 2010;49:9866-73.
4. Lund-Katz S, Hammerschlag B and Phillips MC. Kinetics and mechanism of free cholesterol exchange between human serum high- and low-density lipoproteins. *Biochemistry.* 1982;21:2964-9.
5. Davidson WS, Heink A, Sexmith H, Melchior JT, Gordon SM, Kuklennyik Z, Woollett L, Barr JR, Jones JI, Toth CA and Shah AS. The effects of apolipoprotein B depletion on HDL subspecies composition and function. *J Lipid Res.* 2016;57:674-86.
6. Xu B, Gillard BK, Gotto AM, Jr., Rosales C and Pownall HJ. ABCA1-Derived Nascent High-Density Lipoprotein-Apolipoprotein AI and Lipids Metabolically Segregate. *Arterioscler Thromb Vasc Biol.* 2017;37:2260-2270.
7. Yancey PG, de la Llera-Moya M, Swarnakar S, Monzo P, Klein SM, Connelly MA, Johnson WJ, Williams DL and Rothblat GH. High density lipoprotein phospholipid composition is a major determinant of the bi-directional flux and net movement of cellular free cholesterol mediated by scavenger receptor BI. *J Biol Chem.* 2000;275:36596-604.
8. de la Llera-Moya M, Drazul-Schrader D, Asztalos BF, Cuchel M, Rader DJ and Rothblat GH. The ability to promote efflux via ABCA1 determines the capacity of serum specimens with similar high-density lipoprotein cholesterol to remove cholesterol from macrophages. *Arterioscler Thromb Vasc Biol.* 2010;30:796-801.
9. Tchoua U, Gillard BK and Pownall HJ. HDL superphospholipidation enhances key steps in reverse cholesterol transport. *Atherosclerosis.* 2010;209:430-5.
10. Acton S, Rigotti A, Landschulz KT, Xu S, Hobbs HH and Krieger M. Identification of scavenger receptor SR-BI as a high density lipoprotein receptor. *Science.* 1996;271:518-20.
11. Rosales C, Tang D, Gillard BK, Courtney HS and Pownall HJ. Apolipoprotein E mediates enhanced plasma high-density lipoprotein cholesterol clearance by low-dose streptococcal serum opacity factor via hepatic low-density lipoprotein receptors in vivo. *Arterioscler Thromb Vasc Biol.* 2011;31:1834-41.
12. Gillard BK, Rodriguez PJ, Fields DW, Raya JL, Lagor WR, Rosales C, Courtney HS, Gotto AM, Jr. and Pownall HJ. Streptococcal serum opacity factor promotes cholesterol ester metabolism and bile acid secretion in vitro and in vivo. *Biochim Biophys Acta.* 2016;1861:196-204.
13. Radin NS. Extraction of tissue lipids with a solvent of low toxicity. *Methods Enzymol.* 1981;72:5-7.